Oceanologia 63 (2021) 403—419

Available online at www.sciencedirect.com

ScienceDirect

journal homepage: www.journals.elsevier.com/oceanologia

ORIGINAL RESEARCH ARTICLE

Role of riverine inputs, low saline plume advection and mesoscale physical processes in structuring the Chlorophyll *a* distribution in the western Bay of Bengal during Fall Inter Monsoon

Jagadeesan Loganathan[a,*], Rao Darapu Narasimha[a], Ignatious Joseph[b], AswinDev Meleth Parambil[b], Vivek Rachuri[a], Behera Swarnaprava[a], Balachandran Kizhakkepat Kalathil[c]

[a] *CSIR — National Institute of Oceanography, Regional Centre, Visakhapatnam, India*
[b] *School of Ocean Science and Technology, Kerala University of Fisheries and Ocean Studies, Panangad, India*
[c] *CSIR — National Institute of Oceanography, Regional Centre, Kochi, India*

Received 2 February 2021; accepted 28 April 2021
Available online 20 May 2021

KEYWORDS
River influx;
Low saline plume advection;
Mesoscale eddy;
Chlorophyll *a*;
Double chlorophyll maxima;
Bay of Bengal

Abstract This study delineates the role of small and medium river inputs, Low Saline Plume Advection (LSPA) and eddies in hydrography alteration and Chlorophyll *a* (Chl. *a*) in the Western Bay of Bengal. Samples were collected across five transects viz: Hooghly (HO), Mahanadi (MN), Rushikulya (RK), Visakhapatnam (VSKP) and Godavari (GD) during Fall Intermonsoon. Each transect consists of 7 or 8 locations from inshore to offshore. LSPA propagates southward concordance with the East India Coastal Current (EICC) and its southward flow strengthened by a cold-core eddy. LSPA results in the intermittent low salinity in the cross-shore section of HO, MN and RK. Upper layer Chl. *a* is 2—3 folds higher in inshore and in LSP-influenced locations than in its adjacent stations. The present study identified Double Chlorophyll *a* Maxima (DoCM) in LSPA-influenced slope regions of MN and RK. DoCM is less known in the BoB. DoCM has both the Surface Chl. *a* Maxima (SCM) and Subsurface Chl. *a* Maxima (SSCM). SSCM layer is relatively shallow and intense in slope and offshore regions of MN and RK due to their closeness with

* Corresponding author at: CSIR — National Institute of Oceanography, Regional Centre, Visakhapatnam, India.
E-mail address: jagadeesanl@nio.org (J. Loganathan).
Peer review under the responsibility of the Institute of Oceanology of the Polish Academy of Sciences.

Production and hosting by Elsevier

https://doi.org/10.1016/j.oceano.2021.04.004

cold-core eddy. The present study highlights that freshwater discharge from small and medium rivers impacts hydrobiology around 10—50 km from the shore depends on the magnitude of river influx. LSPA is away from the local inputs and impacts hydrobiology (>500 km) along the path. EICC and eddies together regulated the direction of LSPA. Existing eddies nature alters vertical hydrobiology in slope and offshore regions.

1. Introduction

The mixed layer dynamics of Bay of Bengal (BoB) is unique and it is controlled by several factors such as cyclones, clouds, solar irradiance, eddies, upwelling, coastal currents, precipitation, river runoff etc. (Gomes et al., 2000; Jyothibabu et al., 2015; Madhupratap et al., 2003; Madhu et al., 2006; Paul et al., 2008; Prasanna Kumar et al., 2002; Prasanna Kumar et al., 2004). BoB receives an enormous quantity of freshwater through precipitation and river runoff (1.6×10^{12} m^3 y^{-1}) (Bharathi et al., 2018; Rao and Sivakumar, 2003; Subramanian, 1993). The freshwater flow considerably reduces the surface salinity of the Bay of Bengal, which is evident as Low Saline Plume (LSP) in the Northern Bay of Bengal (NBoB). Ganges and Brahmaputra are the major rivers, while there are also medium rivers debouching into the northwestern (Mahanadi, Hydri and Vamshadara) and southwestern (Krishna, Godavari, Caveri) bay (Sarma et al., 2012; Subramanian, 1993). Freshwater influx (~15000 m^3 s^{-1} in Ganges, 638 m^3 s^{-1} in Mahanadi, 111 m^3 s^{-1} in Vamsadara and 1600 m^3 s^{-1} in Hydri) extend the estuarine characteristics to several kilometres of offshore in the NBoB. Previous studies from BoB (Bharathi et al., 2018; Gomes et al., 2000; Madhupratap et al., 2003; Paul et al., 2008; Prasanna Kumar et al., 2004) majorly considered Ganges and Brahmaputra riverine inputs for evaluating the freshwater impact on the hydrography and biological production. Small and medium rivers bring nutrients and influence phytoplankton production of near shore and coastal waters (Baliarsingh et al., 2015; Baliarsingh et al., 2016); however, the actual role of small and medium rivers on hydrobiology is overlooked in BoB.

Seasonally reversing East India coastal current (EICC) influences the hydrography and biological production in BoB (Jagadeesan et al., 2019; Jyothibabu et al., 2015). EICC flow is poleward during Spring Intermonsoon (SIM) and equatorward during the Winter Monsoon period. EICC carries the low saline BoB waters in their path and joins with the Winter Monsoon current and transfers the low saline waters into the Arabian Sea during the Winter Monsoon period (Shankar et al., 2002; Shenoy, 2010). Late Southwest Monsoon and Fall Intermonsoon (FIM) is a transition period; EICC is weak and equatorward in the northern Bay of Bengal (Shankar et al., 2002). LSP advected towards the south (along the coast up to 18°N) by EICC (Amol et al., 2019; Shetye et al., 1991; Shetye, 1993; Vinayachandran and Kurian, 2007) and Low Saline Plume Advection (LSPA) path is away from the local inputs (Shetye et al., 1991). This kind of LSPA may significantly impact the hydrography and biological production in their influenced location along the path, but the actual quantification of LSPA on hydrobiology is meager in BoB.

Mesoscale eddies are common in BoB (Jagadeesan et al., 2019; Prasanna Kumar et al., 2004; Sarma et al., 2018). Based on the nature of circulation, eddies are classified into cold-core and warm-core eddy. Eddies alter the column hydrography and biological production in their path (Jagadeesan et al., 2019; Mahadevan et al., 2012; Paul et al., 2008). Cyclonic eddies pumping the nutrients into the euphotic water column and increases the biological production compared to non-eddy or warm-eddy conditions (Fernandes and Ramaiah, 2009; Jagadeesan et al., 2019; Paul et al., 2008; Prasanna Kumar et al., 2004). During the Southwest Monsoon (SWM) period, warm-core eddy/gyre was reported in south of the 18°N and few cold-core eddies in the north of the 18°N (Prasanna Kumar et al., 2007). Coastalward eddy in the northwestern Bay of Bengal could influence the horizontal propagation, path and speed of low saline plume advection and vertical structure of hydrography during the FIM.

We hypothesize that equator flow of the low saline plume (LSP), local river inputs and mesoscale eddies altogether influence the spatial and vertical distribution of Chl. *a* in the WBoB. These processes' existing space has differed, for delineate each process role in hydrobiology alteration required cross-shore sectional studies. Past studies from nearshore waters and coastal waters of the BoB are predominantly the spot measurements (Baliarsingh et al., 2015; Baliarsingh et al., 2016; Choudhury and Pal, 2011; Naik et al., 2020) and cross-shore sectional studies (Bharathi et al., 2018; Gomes et al., 2000) missed out the information about local rivers and the LSPA impact on hydrography. In the present study, hydrographic observations are carried across five transects [Hooghly (HO); Mahanadi (MN); Rushikulya (RK); Visakhapatnam (VSKP) and Godavari (GD)] during the FIM period to explain the following objectives in the WBoB Viz., 1) study the influence of southward propagation of LSP on the hydrobiology; 2) delineate the role of small and medium rivers and LSPA on the hydrography and Chlorophyll *a* distribution; 3) study the role of EICC and mesoscale eddies on the horizontal extension of LSPA and vertical distribution of hydrography and Chlorophyll *a* distribution.

2. Material and methods

2.1. Sampling and methods

The sample collection was onboard r/v *Sindhu Sankalp (*SSK 105) from 5 cross-shore transects during 21 September—4

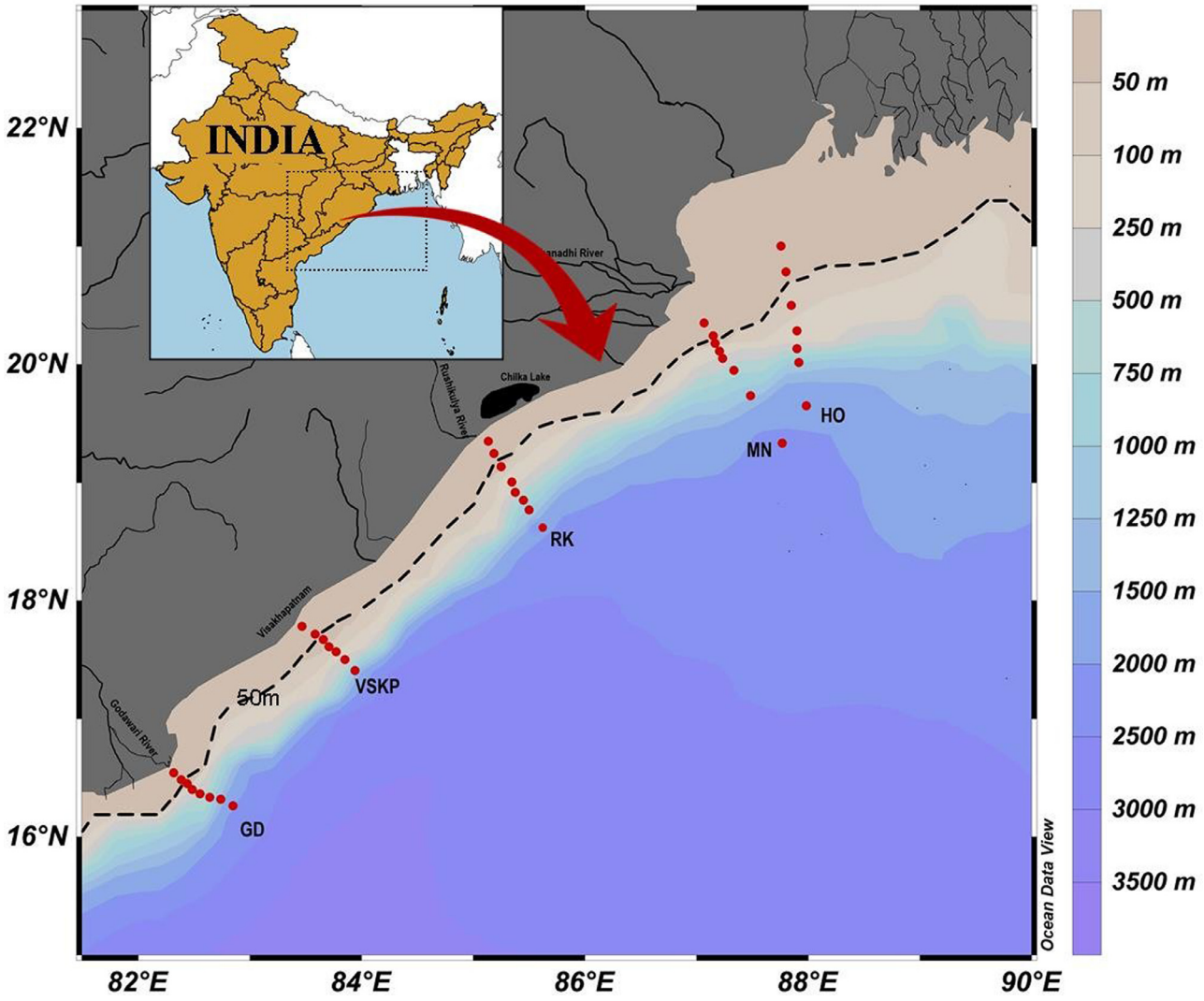

Figure 1 Study area. Cross-shore transects of the present study [Hooghly (HO); Mahanadi (MN); Rusikulya (RK); Visakhapatnam (VSKP); Godavari (GD)]. Scale Bars: depth contours. Dotted line represents 50 m depth contour.

October 2017 (Figure 1). Altogether, this study spatially covers ~800 km from the north. Cross shore sectional coverage varied between 75 km and 230 km. Each transect has 7 to 8 stations and the depth of the locations ranging from 25 to 2000 m. Based on the depth, sampling locations classified into inshore (station 1; 25 m), near coast (station 2; 50 m), coastal (Station 3; 100 m), slope (stations 4—6; 250—1000 m) and offshore (stations 7 and 8; 1500—2000 m). Hooghly transect (HO) is 60 km away from the extreme north. Mahanadi transect (MN) is 100 km south of HO; Rushikulya (RK) is 230 km south of MN. Visakhapatnam is 240 km south of RK; Godavari (GD) is 180 km south of Visakhapatnam.

Vertical salinity and temperature measured through rosette Sea-Bird CTD (Conductivity, Temperature and Depth profiler). WET Labs ECO-AFL/FL (Fluorometer) and WET Labs ECO-NTU (Turbidity meters) were fitted with CTD rosette for measuring the vertical pattern of the Chlorophyll *a* and turbidity. For explaining the hydrography of the entire basin, near real-time satellite merged sea level anomalies, geostrophic currents, Chlorophyll *a* and salinity (predicted model for forecast) were retrieved from Copernicus data source (http://marine.copernicus.eu) and plotted as 2D colour maps using ODV 4.7 (http://odv.awi.de/). Water samples were collected for estimating dissolved oxygen, nutrients and phytoplankton biomass using Niskin samplers from 4 to 8 discrete different depths (0, 5, 10, 25, Subsurface Chlorophyll *a* Maxima layer, 50, 75 and 100 m) depends upon the depth of the water column. Dissolved oxygen measured through Winkler's method using Tritrinado 835 Metrohm auto titrator. Nutrients (nitrate, phosphate and silicate) analysed onboard using calibrated advanced instruments like SYSTEA μMAC 1000 and Green Eyes EcoLAB (Grasshoff, 1983).

For measuring the Chlorophyll *a*, 2 L of the water samples filtered through the GF/F filter paper (47 mm diameter) with a mild vacuum (<100 mm Hg). Filter papers were wrapped in aluminium foil, placed in small cryo vials (2 ml) and stored in liquid nitrogen till analysis. In the laboratory, the Chl. *a* in the phytoplankton cells were extracted overnight using 90% acetone and incubated in the dark at 4°C and measured using the calibrated Turner designed Fluorometer (UNESCO, 1994). Chlorophyll *a* obtained

from Ecolab's Fluorometer was corrected with the lab measured Chl *a* using the regression equation (Corrected Chl *a* = 1.13 + 0.08 × CTD Chl *a*; r = 0.92; p <0.01; N= 228) for high resolution representation.

Integrated Chl *a* was calculated following Dyson et al. (1965)

$$\text{Integrated Chl } a = [(d_1 - d_0)(a_0 + a_1)/2 + (d_2 - d_1)(a_1 + a_2)/2 + \ldots]$$

Where d_0, d_1, d_2 are the depths sampled, and a_0, a_1, a_2 are the Chl. *a* of the respective depths.

Integrated Chl. *a* calculated surface − 25 m, surface − 50 m and surface − 100 m in inshore, near shore and coastal stations respectively. However, upper 100 m depth layers only used in slope and offshore locations for calculating the Integrated Chl. *a*. For comparing Chlorophyll *a* accumulation in various depth layers, the integrated Chl. *a* was calculated at every 10 m.

2.2. Univariate and multivariate analysis

Hydrographical parameters difference within and between transects compared through parametric (one way) or non-parametric (Kruskal Wallis) ANOVA depends upon the distribution of data set (Zar, 1999). Multivariate Redundancy Analysis (RDA) performed to find out the interrelationship between the hydrographical parameters and Chlorophyll *a* distribution. Two sets of RDA (upper layer and column layers) performed to delineate the impact of the various processes associated with hydrography alterations on Chl. *a* distribution. Upper layer RDA, entire sampling stations were considered to perform RDA; however, inshore and near coastal locations were omitted in column RDA due to their shallow depth. RDA performed as per the standard procedure of Leps and Smilauer (2003) using CANOCA version 4.5. RDA ordination significances were tested with the Monte Carlo permutation test.

3. Results

3.1. Coastal currents and salinity

Low saline waters occupied in the northwestern BoB during the Late SWM period (Figure 2) associated with the riverine flux. Geostrophic currents pattern visualised, EICC flow has changed southward during the third week of September but the flow is disorganised. LSPA propagates southwards along with the EICC is evident in Figure 2. Concurrently, there is a cold-core eddy found between 19.5°N and 17.22°N (core at 86.5°E 18.32°N), with a spread of 120 km towards the shore. EICC joins with the eddy's western arm at ∼20°N and strengthens the southward advection of LSPA along HO, MN and RK transect. South of RK (∼18°N) transect, LSPA is deflected towards the offshore (Figure 2) by cold-core eddy. During the present study period, LSP was 120 km away from the coast at HO, but moved further closer to the coast in the south of HO.

3.2. Upper layer hydrography

Insitu salinity showed a close resemblance with satellite-derived salinity. Salinity gradually increased from inshore to offshore in GD, but this wasn't similar in other transects. LSPA results the intermediate low salinity in the cross-shore section of HO, MN, and RK transect. LSPA considerably lowered the upper layer (surface − 10 m) salinity in their path. LSPA was ∼120 km away from the coast and ∼70 km wider in HO. Near coast (station 2) and coastal station (station 3) faced influence of LSPA and salinity was 3 to 11 units less compared to the adjacent inshore (station 1) and slope (station 4) in HO (Figure 3). Towards the south, LSPA was relatively closer to the coast than HO. LSPA was 60 km far from the coast and 55 km wide in MN transect. LSPA impacts the slope location (stations 4–6) of MN transect and it reduces salinity (4.8 to 7.8 units) compared to neighbouring stations. LSPA was 40 km away from the coast and ∼55 km wide in RK transect. Coastal (station 3) and slope regions (stations 4 and 5) faced LSPA and found 0.5–5 salinity less compared to adjacent locations (Figure 3). Salinity in GD transect was relatively high compared to all other transects (Figure 4). VSKP transect intermittent low salinity found in the location 4 and 5 (slope), but this was in a thin layer (∼5 m), probably caused by the LSPA advection due to cold-core eddy.

LSPA influenced locations were relatively warm (0.5°C–1°C) and highly oxygenated (0.5 to 2.8 ml L^{-1}) compared to their adjacent regions. Upper layers along the HO, MN and RK were relatively oxygenated compared to GD (Figures 3 and 4). Turbidity in the upper layer differed within and between transects. In general, inshore and LSPA influenced areas were relatively turbid compared to other locations. Irrespective of transects, offshore regions were fairly transparent compared to inshore regions. Nutrients concentration (nitrate and phosphate) in upper layers (0–10 m) is found <1.5 μM in the entire study locations (Figure 5). Nitrate concentration was relatively high in inshore and LSPA influenced locations, indicating that local inputs and LSPA influencing the upper layer nutrients (Figure 5). Phosphate concentration is slightly low in along the path of LSPA compared to adjacent locations. Upper layer nutrients didn't show any significant elevation during the study period.

3.3. Column hydrography

Water column hydrography exhibited wide fluctuations between transects response to the variability in the physical forcing. Vertical profile of temperature and dissolved oxygen shows that the subsurface waters relatively warm and oxygenated in GD compared to the northern transects. Offshore region, 25°C isotherm and hypoxic depth (1.4 ml L^{-1}) were shallow (45–60 m) in the HO, MN and RK, while it was much deeper (70–90 m) in GD transect. The trend is maintained even at 100 m depth; water columns were 3.9–5.4°C cooler and oxygen-deficient in HO, MN and RK compared to the GD. Hydrographical parameter differences between slope and offshore regions of HO, MN and RK were noticeable; however, slope to offshore variations was minimal in GD. Subsurface layers (40–100 m) were relatively cool and

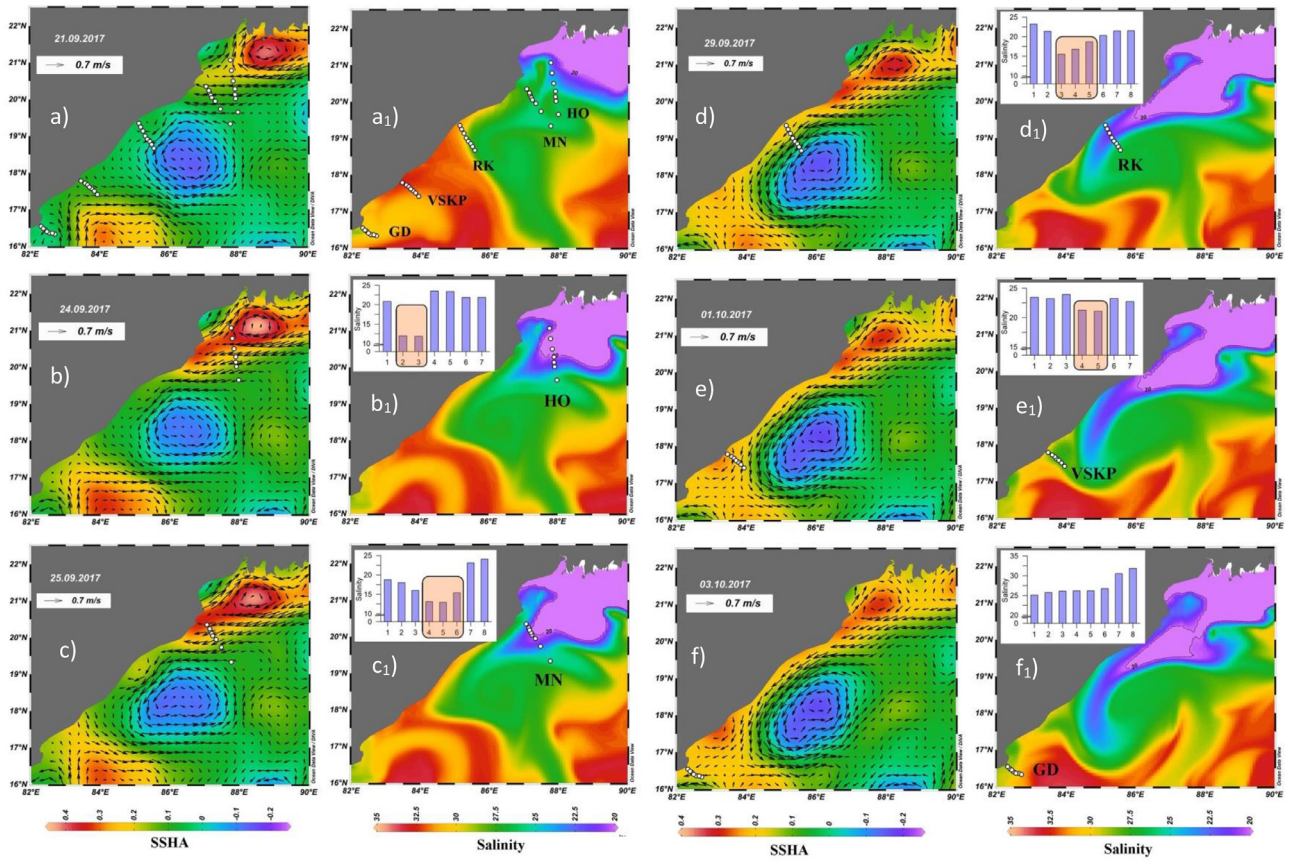

Figure 2 Sea surface height anomaly (SSHA) (column 1 and 3) overlaid on satellite-derived geostrophic currents, salinity (Spatial contour plots — column 2 and 4) during the 3rd week of September to the first week of October 2017. Measured surface salinity is inserted as bar charts indicating the spatial difference during the sampling period. Figure a and a_1 represent SSHA anomaly and salinity condition in the Western Bay of Bengal on the 21st September (3 days before sampling), subsequent plots mentioned date and white dots represent the sampling locations at that particular period of sampling. Low saline waters are occupied in the extreme northern locations before the sampling period. Low saline plume begins propagates towards the south during our sampling period response to the EICC and advected into further south as the combined action of EICC and coastal ward periphery of the cyclonic eddy. LSPA was away from the coast and well separated from the local inputs was evident by the intermittent low salinity in cross shore sections of the HO, MN and RH. LSP is passing through the coastal locations of HO, slope locations of MN and, coastal and slope locations of RK. Advection of LSP is ∼120 km away from the coast in the north, while it is closer to coast towards the south (60 km at MN and 40 km at RK); South of RK (∼18.25°N), LSP is advected towards offshore by the southern arm of the cold core eddy.

less oxygenated in offshore regions of HO, MN and RK compared to the slope. At 100 m depth contour, temperature showed a large thermal gradient (2—5°C) between the offshore and slope waters along HO, MN and RK, while it was $<$ 1.5°C in VSKP and $<$ 0.5°C in GD transect (Figure 3 and 4). Dissolved oxygen also showed a similar gradient, 4—5 folds less in offshore regions of HO, MN and RK than the slope; however, offshore was relatively more oxygenated than slope regions of VSKP and GD (Figure 3 and 4). In the subsurface layer (50, 75 and 100 m), nutrients were relatively high in offshore compared to slope regions in RK, MN and HO transect (Figure 5). Vertical distribution of temperature, DO and nutrients attributed to the fact that up slopping was prominent along the offshore regions of HO, MN and RK due to their close association with cold-core eddy.

3.4. Chlorophyll *a* distribution in upper layers

Chlorophyll *a* showed a significant spatial difference between transects due to changes in hydrographical conditions (Figure 6). Spatially, Chl. *a* varied from 0.2 to 6 mg m^{-3} in upper layers, high values found along the HO, MN and RK transect compared to the GD. Chl. *a* was high in inshore and LSP influenced locations compared to offshore waters. Offshore water Chl. *a* levels were more or less uniform. Along the HO transect, the surface Chl. *a* was 2—3 folds high in LSP influenced near coast and coastal location compared to the adjacent slope and inshore. MN transect, Chl. *a* was relatively high in the inshore region, which decreased towards the coastal region and found the intermittent high in LSPA influenced the slope location (locations 4—6). RK transect also, Chl. *a* was high in the inshore region and LSPA influ-

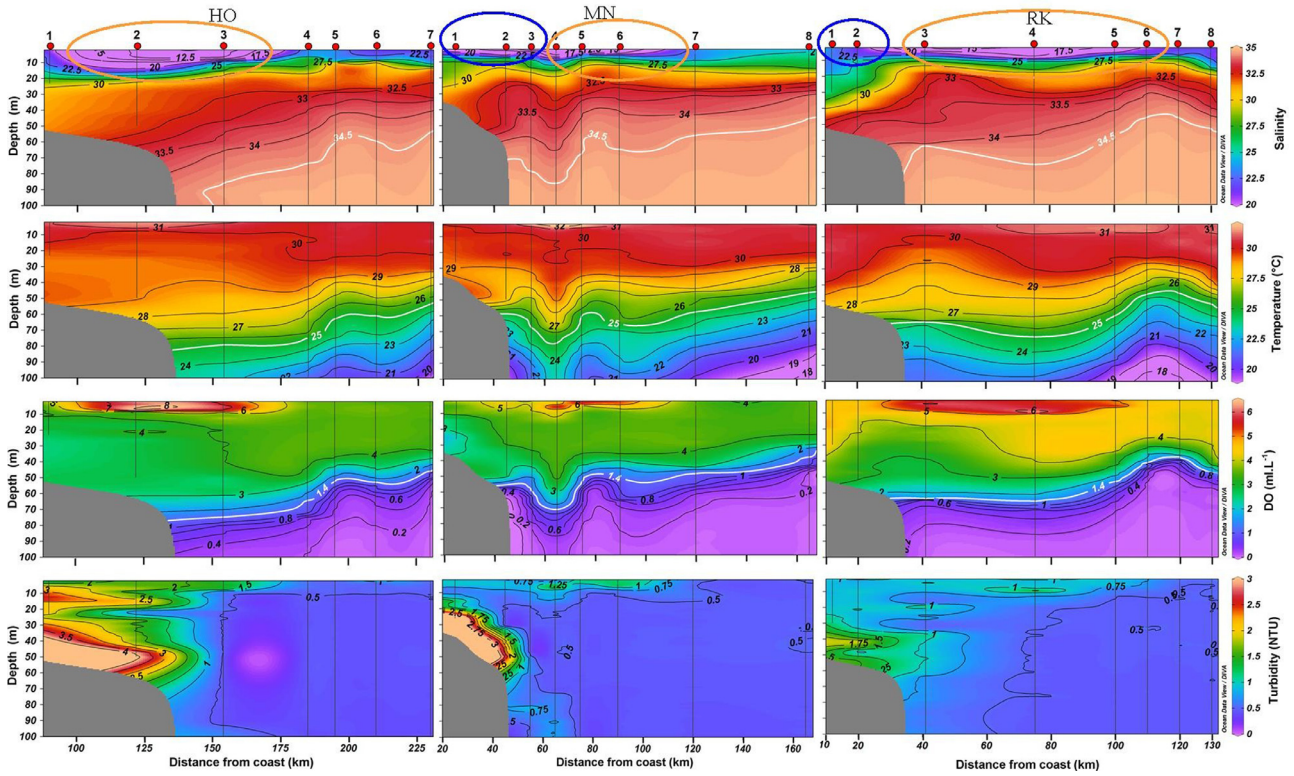

Figure 3 Distribution of salinity, temperature, dissolved oxygen and turbidity across Hooghly (HO), Mahanadi (MN) and Rusikulya (RK) transects. The blue circle is the region influenced by freshwater input from small and medium rivers, while the orange circle is the region influenced by Low Saline Plume Advection (LSPA). Near coast (station 2) and coastal (station 3) location in HO, slope locations 4,5, 6 in MN, coastal and slope locations in RK are influenced by Low saline Plume Advection (LSPA). LSPA influenced locations upper layer is characterized as low saline, warm and oxygenated compared to adjacent inshore and slope regions. Up slopping of temperature (T25°C), salinity (34.5) and hypoxic layer (dissolved oxygen —DO: 1.4 ml L^{-1}) is prominent in offshore across HO, MN and RK transect, while it is relatively deeper in the slope locations. Turbidity was spatially high in inshore to coastal locations compared to offshore locations. LSPA influenced location turbidity was relatively high compared to adjacent locations.

enced coastal and slope regions (Figure 6). VSKP transect Chl. *a* was weak close to the coast and it increased in location 4 and 5 related with the advective effects of LSP along the southern arm of the cold core eddy. GD transect Chl. *a* was less compared to the northern transects.

3.5. Vertical distribution of Chlorophyll *a*

Vertical distribution of Chl. *a* along the northern transects were significantly different from the GD. Subsurface Chlorophyll *a* Maxima (SSCM) layer was shallow with a high concentration in northern transects compared to GD. SSCM was relatively deeper, but less concentration in LSPA influenced slope locations of MN and RK (Figure 6 and 7) than offshore. Inshore regions, the integrated Chl. *a* was high in MN compared to other transects. In upper layer (0—10 m) integrated Chl. *a* in LSPA influenced shelf and slope regions were 3 to 6 folds higher compared to adjacent location. Offshore upper layers integrated Chl. *a* concentration was comparable between northern and GD, but it significantly differed in subsurface layers. SSCM was relatively shallow (30—50 m) and prominent in the north transects compared to VSKP and GD (Figure 6 and 8).

Based on the Chl. *a* distribution, three types of Chl. *a* pattern recognized in the study region (Figure 7), i.e., 1) Surface Chlorophyll *a* Maxima (SCM), 2) Subsurface Chlorophyll *a* Maxima (SSCM) and 3) Double Chlorophyll Maxima (DoCM). High Chl. *a* in the upper layer of inshore, near coast and coastal waters were denoted as Surface Chlorophyll *a* Maxima. 2) High Chl. *a* in the subsurface (40—80 m) layers along the offshore region, denoted as SSCM; 3) Double Chlorophyll maxima (DoCM). DoCM has two high Chl. *a* layers. The first maxima is located in the upper layer (0—10 m) while the second maxima in the subsurface (50—80 m) layer, intermediate low Chl. *a* layer separates both. In the present observation, DoCM was observed in LSPA influenced slope locations of MN and RK transect (Figures 6 and 7). The SCM and SSCM were well recognised in the BoB, whereas a DoCM is less known, which needs further investigations to corroborate. Chl. *a* concentration in the SSCM layer was comparatively less in slope regions than the offshore along the transects of HO, MN and RK.

3.6. Interrelationships between the phytoplankton production and environmental parameters

Interrelationships between the Chl. *a* and hydrographical parameters were assessed through Redundancy analysis (RDA). Altogether, hydrographical parameters explained

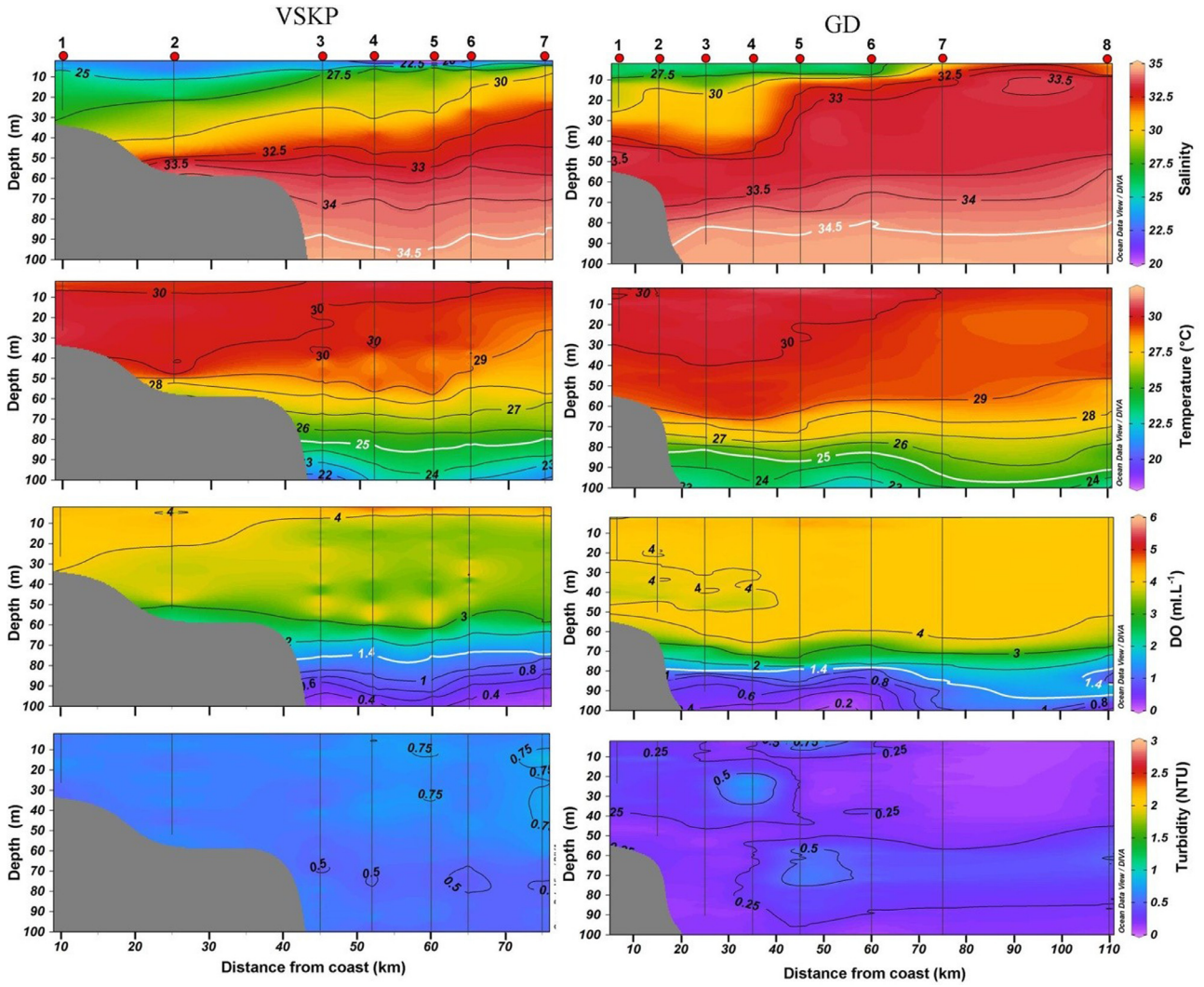

Figure 4 Distribution of salinity, temperature, dissolved oxygen and turbidity across Visakhapatnam (VSKP) and Godavari (GD) transect. Isolines of T25°C, salinity 34.5 and hypoxic layer is relatively deeper in the GD transect compared to the northern transect (see Figure 3). Slope to offshore differences of salinity, temperature and dissolved oxygen was comparable in the GD transect. Upper layer salinity is relatively high in the GD transect than the other transects.

74.63% variation of the Chl. *a* distribution, in that first two axes explained 70%. Monte Carlo permutation test results show that the RDA pattern was significant (499 unrestricted permutations) ($p < 0.05$).

3.6.1. Upper layer RDA

Salinity was oriented left-hand side of the RDA plot. Temperature, DO, Turbidity and nutrients were oriented right side of the plot represents their affirmative relationship with each other and inverse relationship with salinity (Figure 9). The negative gradients of the salinity and positive gradients of the temperature, DO, turbidity, and nutrients along with LSPA and small and medium river influenced locations of MN, HO and RK transect represent the significant role of LSPA and local inputs in hydrographical variations in the Bay of Bengal. LSPA influenced locations assembled in the upper portions of the right-hand side. The inshore and coastal waters of north transects assembled in the lower portions of the right side represent their differentiation. LSPA influenced locations characterised as comparatively warm, oxygenated than the inshore and coastal locations was evident with their closeness of temperature and DO axes (Figure 9). Noticeably, nitrate concentration didn't show any significant pattern between the LSPA influenced location and local inputs. Offshore locations grouped in the left-hand side of the plot, characterised as high saline with relatively cool and less oxygenated compared to local inputs and LSPA influenced locations. Chl. *a* concentration in the surface layer and integrated Chl. *a* concentration oriented right side of the plot along with increasing gradients of the temperature, DO, nutrients and turbidity but reverse direction to salinity represent that the LSPA and local inputs increased the Chl. *a* concentration in upper layers significantly.

3.6.2. Water column characteristics RDA

Orientation of hydrographical parameter axes visualised the hydrography differences between transects (Figure 9). Axes

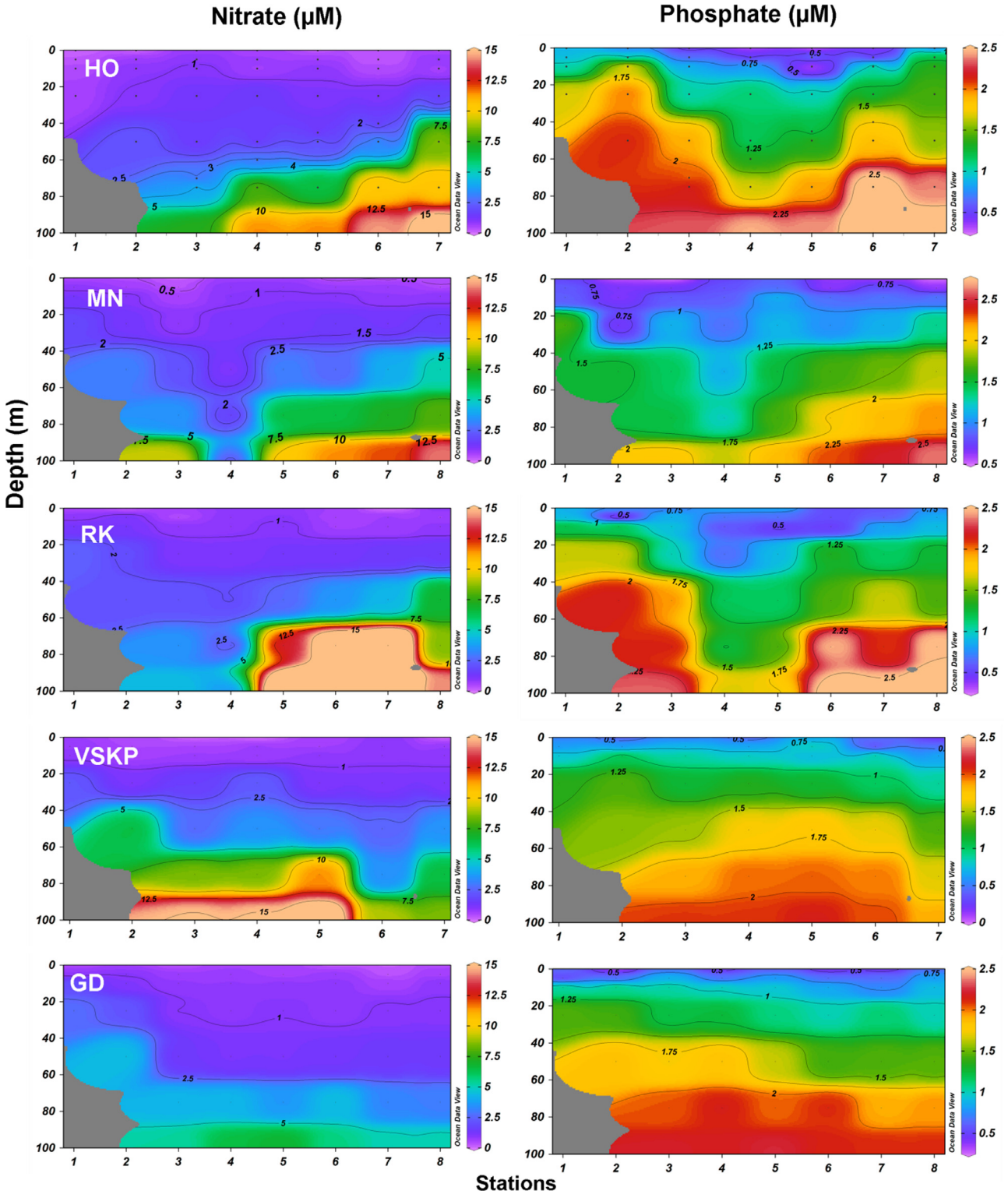

Figure 5 Spatial and vertical distribution of the Nitrate and Phosphate across the transects of HO, MN, RK, VSKP, GD. There is a significant difference in the subsurface nutrients within and between transects. Nutrients concentrations in subsurface layers are relatively high in northern transects compared to GD. Along the northern transects, up slopping of the nutrients were prominent in slope to offshore locations.

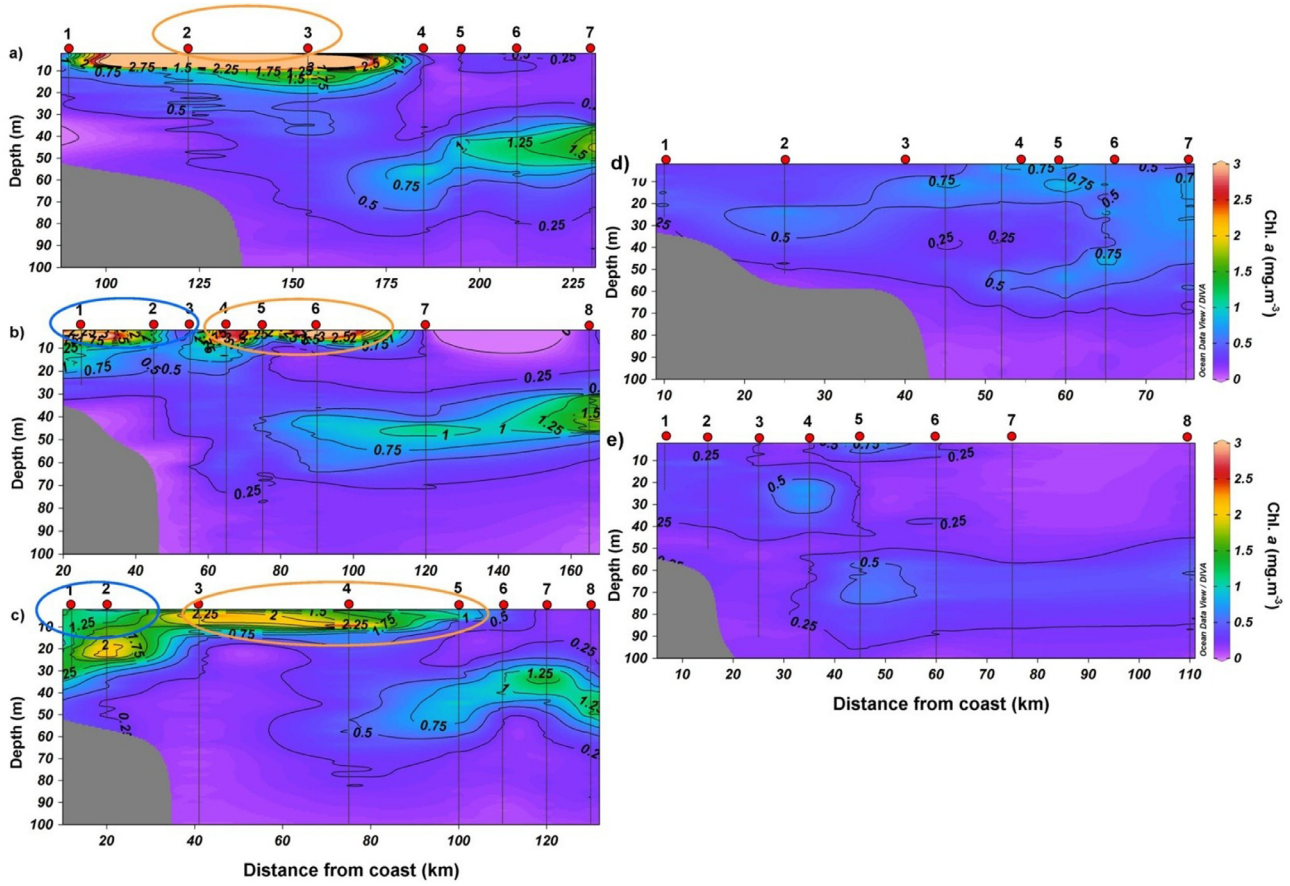

Figure 6 Distribution of chlorophyll *a* across a) HO b) MN c) RK d) VSKP and e) GD transects. Blue circles are region influenced by freshwater input from small and medium rivers, while orange circles are region influenced by low saline plume advection (LSPA). It is evident that the high surface Chl. *a* in the inshore and near coastal areas are caused by small and medium rivers, while the high surface Chl. *a* in the offshore regions are caused by LSP. In the northern bay, the coastal region has a prominent surface Chl. *a* maxima (SCM), while the offshore region has a prominent subsurface Chl *a* maxima (SSCM). The SSCM in the northern bay is relatively shallow and intense compared to the southern bay (GD). Most importantly, the LSP influenced slope regions (MN, RK transects) have Double Chl *a* maxima (DoCM) which consists of two high Chl. *a* layers (surface and subsurface) separated by an intermittent layer of low Chl *a*. Noticeably, Chl. *a* in SSCM is relatively low in LSP influenced (slope) regions compared to offshore locations.

of surface salinity, subsurface layer temperature and dissolved oxygen oriented left-hand side of the plot with close assemblages with GD transect; whereas the axes of surface temperature, dissolved oxygen and nutrients (surface and subsurface layers) oriented in the right-hand side of the plot along with the north locations (Figure 9). HO, MN and RK transect characterised as relatively warm, low saline and oxygenated in surface layers compared to GD; but cool, less oxygenated and nutrient-rich in subsurface layers. Orientation of the hydrographical parameters axes represent that freshwater advection and existing mesoscale physical processes differed between north and GD. LSPA influenced slope locations assembled in the lower portion of the right-hand side. Offshore locations grouped in the upper portions of the right-hand side represent slope to offshore hydrography differences within northern transects. Upper layer Chl. *a* axes were oriented with the close affinity to the surface DO and temperature axes with LSPA influenced locations indicate LSPA advection enhances the upper layer hydrography in their influenced coastal and slope locations. Subsurface layer Chl. *a* axes had a close affinity with the subsurface nutrient axes, and opposite direction to the DO axes with offshore locations represents the up sloping of nutrients by cold-core eddy closeness enhances the Chl. *a* in RK and MN. Chlorophyll *a* axes of the 80 m oriented left-side of the plot with the positive gradients with subsurface dissolved oxygen layer along with GD represents down slopping features deepening SSCM layer in GD compared to north transects (Figure 9).

4. Discussion

Northern Bay of Bengal receives the massive outflow from Ganges and Brahmaputra, it contributes >60% in the total freshwater influx to Bay, results the LSP in close to the discharge (Amol et al., 2019; Chaitanya et al., 2014; Rao and Sivakumar, 2003; Shetye et al., 1996; Vinayachandran et al., 2002). LSP occupied northernmost regions during the Southwest monsoon period, and it propagated towards the south during the late SWM (Amol et al., 2019; Murty et al., 1992; Shetye et al., 1991; Shetye, 1993; Vinayachandran and Kurian, 2007) consistent with the flow

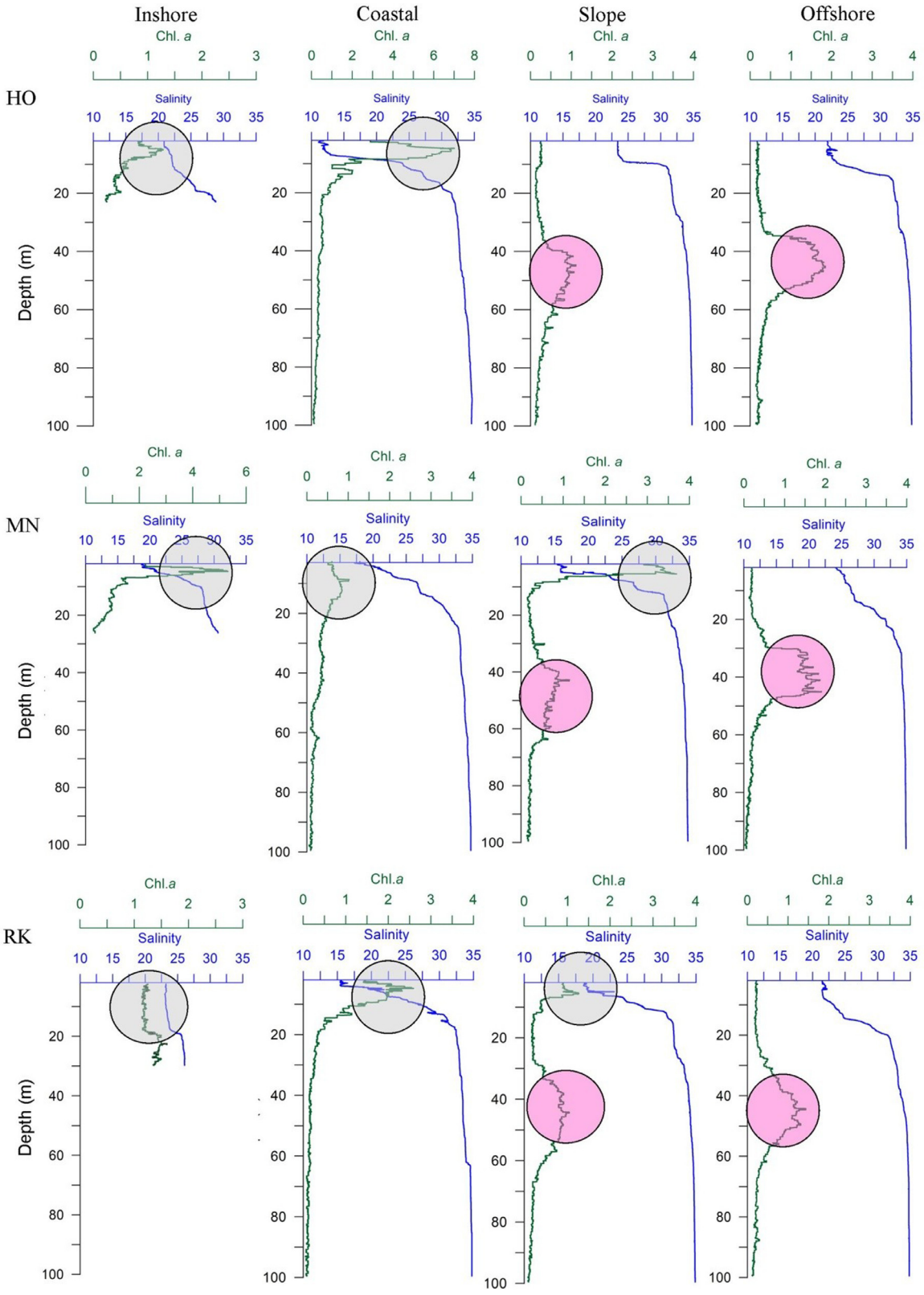

Figure 7 Three patterns of Chl *a* (mg m^{-3}) was identified in relation to salinity along HO, MN and RK transects in the present study. i) high Chlorophyll *a* in surface (SCM) (Grey circles) along the inshore and near coastal waters as the result of freshwater input ii) Subsurface (40—60 m) Chlorophyll *a* Maxima (SSCM) in the offshore region (Pink circle) iii) Double Chlorophyll *a* Maxima (DoCM) identified in low saline plume advection influenced slope regions of MN and RK. DoCM is a less known pattern from the BoB, DoCM has SCM and SSCM both are well separated by a layer of low Chlorophyll *a*.

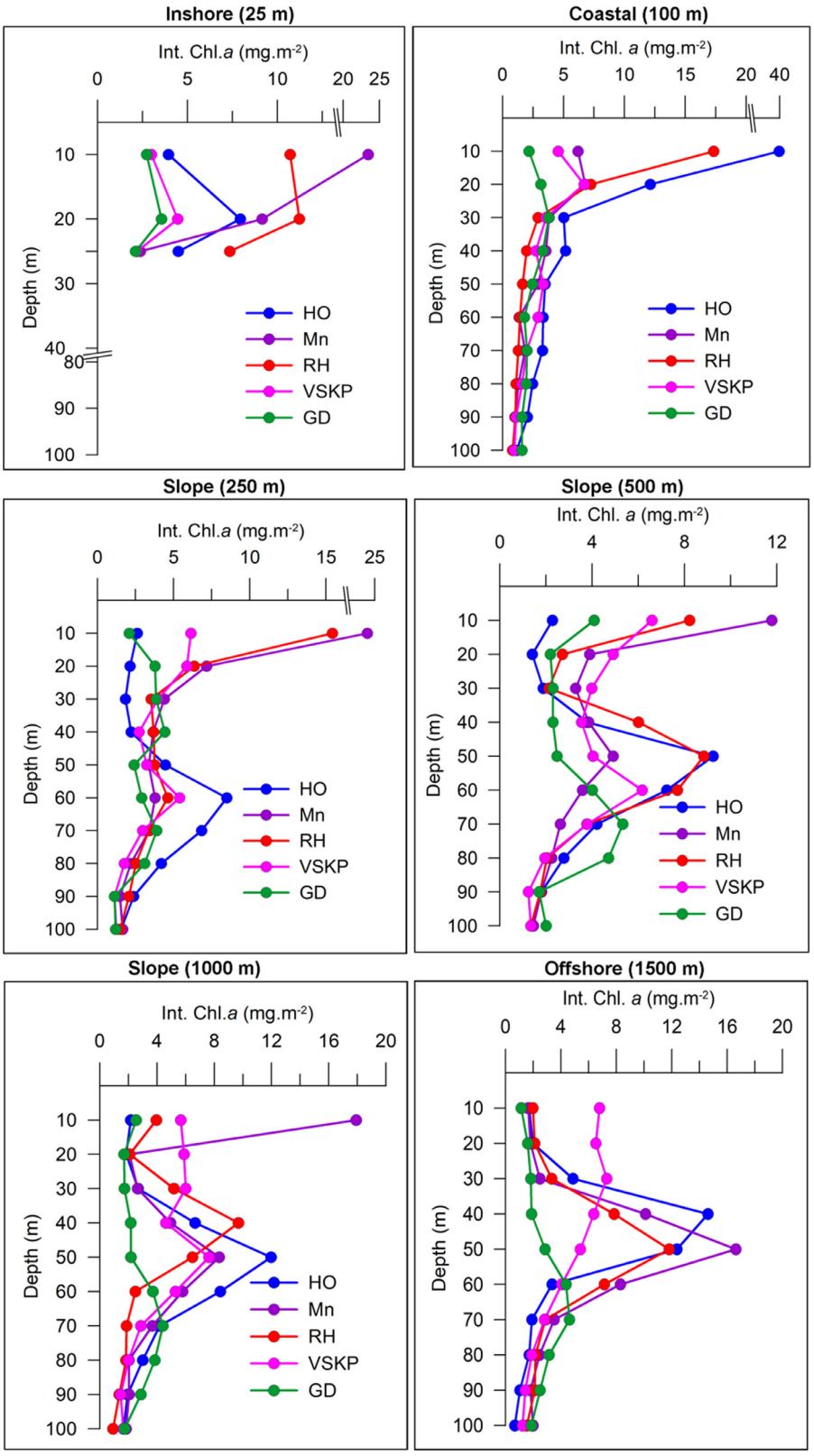

Figure 8 Spatial and vertical distribution of integrated Chlorophyll *a* (every 10 m depth layer) in inshore, coastal, slope and offshore locations. Abbreviations: Hooghly (HO), Mahanadi (MN), Rusikulya (RK), Visakhapatnam (VSKP) and Godavari (GD).

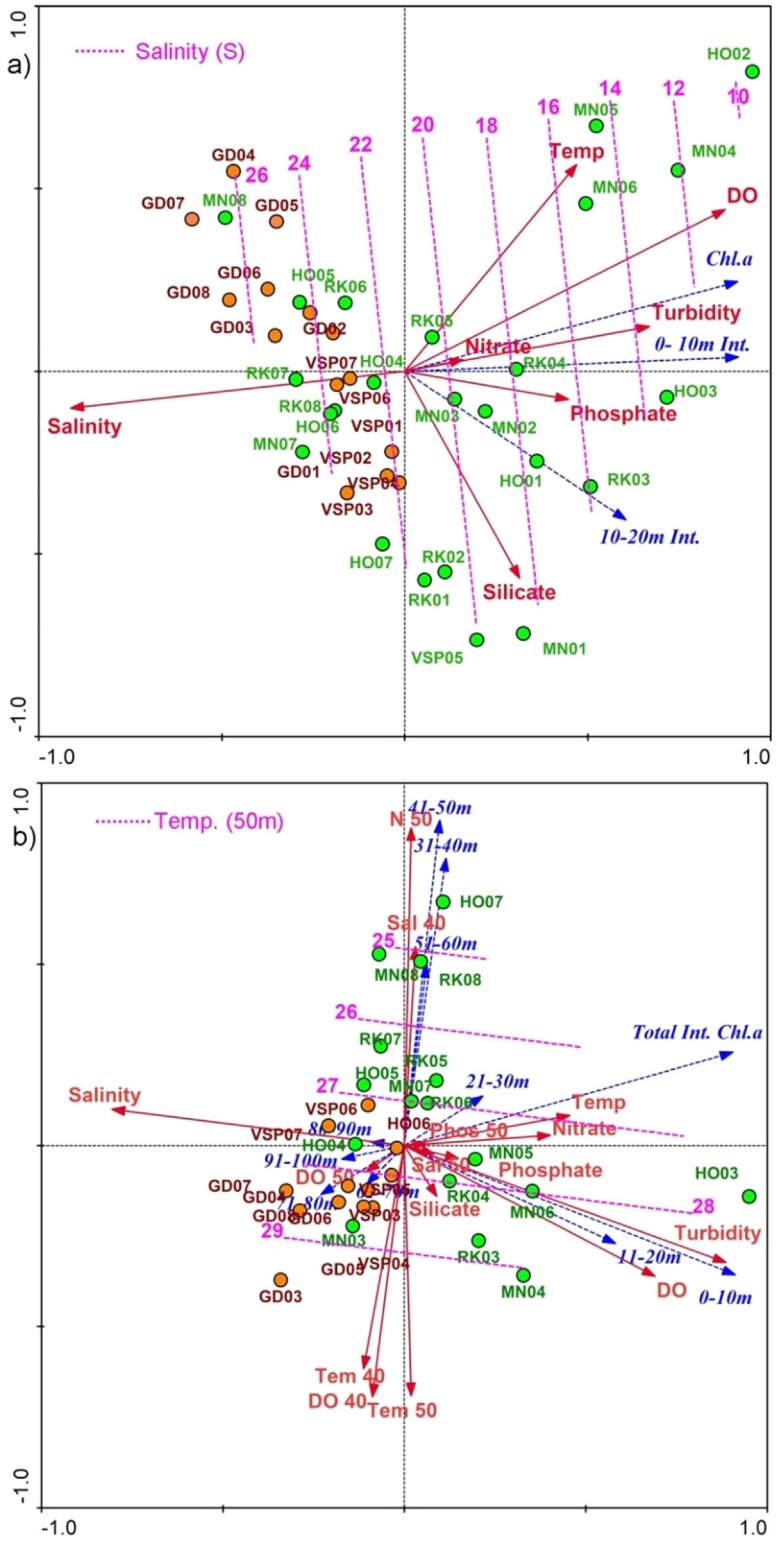

Figure 9 RDA triplot explaining the interrelationships between hydrographical parameters and Chlorophyll *a* distribution. (a) Upper layer RDA triplot and (b) water column RDA triplot. Environmental variables are in the solid red line and biological parameters are in the blue dotted line. Green dots represent the northern locations and orange dots represents the southern transects. The dashed pink line represents the GLM attribution model to represents the spatial pattern of salinity differences between transects in an upper layer and temperature at 50 m depth. Orientation of the hydrographical parameters axes and chlorophyll *a* distribution visualized the spatial heterogeneity of the hydro-biology in upper and subsurface layers associated with local inputs (small and medium river inputs), southward advection of the Low Saline Plume Advection (LSPA) and existing mesoscale physical processes (for more details about the RDA please see the section 3.6 in results).

of EICC (Chaitanya et al., 2014) was evident in Figure 2. The small patch of the low salinity plume up to half of the northwestern Bay of Bengal (upto 17°N) was reported during the late SWM by Shetye et al. (1991). LSPA was confined along the coast and well separated from the coast (Gopalakrishna et al., 2002; Shetye et al., 1991; Vinayachandran and Kurian, 2007). This pattern agreed with the satellite and observational results of salinity in the present study (Figures 2—4). Low saline plume advection is 120 km away from the coast in the extreme north locations, and towards the south, LSPA is relatively closer to coast (60 km far from the coast in MN; 40 km far from the coast in RK). South of RK transect, (∼18.5°N) LSPA advected eastwards offshore (Shetye et al., 1991; Varkey et al., 1996) by the cold core eddy circulations.

Spatially salinity was high in the GD transect compared to northern transects (Bharathi et al., 2018; Sarma et al., 2013). Salinity increased from the inshore to offshore in the GD transect. However, intermittent low salinity in the cross-shore section of the HO, MN and RK transect. Salinity was 0.5 to 11 units less in LSPA influenced locations than their adjacent locations. Similar kind of observation about the intermittent low salinity and salinity gradients between the LSP and adjacent locations reported by Amol et al. (2019); Kusum et al. (2018) and Shetye et al. (1991). Upper layer is differed from the adjacent locations by means of less saline, relatively warm, turbid and oxygenated. LSPA influencing the upper layers (0—10 m) in coastal waters of HO, slope waters of MN and coastal and slope waters of RK transect in their path and results the salinity stratification. Mahanadi river influence on hydrography found upto near coast location (∼50 km) in MN transect but Rushikulya river influence restricts into the inshore location (∼15 km) in RK transect. Riverine inputs alter the hydrography from bar mouth to coastal waters, their extent to offshore depends upon the magnitude of river influx, currents flow (Baliarsingh et al., 2015, Baliarsingh et al., 2016; Choudhury and Pal, 2011; Naik et al., 2020; Sarma et al., 2013).

Inorganic nutrients concentration in upper layers were relatively high in northern transects compared to the south. Inorganic nitrate was found <1.5 μM in upper layers with high vales in inshore, near coast and LSP influenced locations. Sarma et al. (2012) and Sarma et al. (2013) reported glacial river inputs for inorganic nitrate addition in the BoB was less (0.6 ± 0.3 μM) and reported the high nutrients values in the Southwestern regions compared to Northwestern regions. No prominent hike in inorganic nitrate values in LSPA influenced and inshore locations support the view about the significant portions of the inorganic nutrients associated with river flux was utilised within the river system itself (some extend to coastal waters) or high biological consumption by the phytoplankton within coastal waters (Krishna et al., 2016; Sarma et al., 2013). The reported values of the inorganic nitrate and phosphate in the Northwestern Bay of Bengal are comparable with the previous study (Sarma et al., 2012 and Sarma et al., 2013). Letscher, et al. (2013) and Prasad (2014) reported the organic nutrients inputs into BoB through rivers and found higher DON concentrations in coastal waters during the peak discharge period. Studies of the Antia et al. (1991), Moschonas et al. (2017) and Sarma et al. (2019), reported the dissolved organic nitrogen (DON) is an important nitrogen source for phytoplankton and significantly supports the primary production. Comparable levels of inorganic nutrients but high phytoplankton production in LSPA influenced and inshore locations of the northern transects supportive the view about the possible role of DON and Dissolved organic Phosphorous (DOP) for the source of high phytoplankton stock in the BoB but this needs to be examined further.

Warm core situations, down slopping of the salinity and temperature were prominent. Cold-core eddy pumps the cool, nutrient-rich and relatively less oxygenated waters into subsurface layers (Muraleedharan et al., 2007; Prasanna Kumar et al., 2002, Prasanna Kumar et al., 2004; Prasanna Kumar et al., 2007; Sarma et al., 2019). The hypoxic depth and 25°C isotherm (T25°C) were relatively deeper in warm-core situations (GD transect) than cold-core conditions. At 100 m depth layer, offshore location temperature was 3.9—5.4°C less in northern transects and dissolved oxygen concentration was 5—10 folds high in GD transect (Figure 10). Subsurface layer hydrography differed within cross-shore sections of the north transect. Upward pumping in the offshore locations and down-welling reported in the slope locations. These differences between the offshore to slope might be related with distance to cold-core eddy (Figure 2), wind speed, wind stress over the slope regions, underwater circulations, etc., this needs to addressed more detail in physical oceanographic point of view. Irrespective of transects, the turbidity was less in the offshore locations. Turbidity was high in inshore waters associated with the riverine inputs (Bharathi et al., 2018). LSPA influenced locations turbidity, and inshore turbidity was comparable.

Chlorophyll *a* distribution showed a significant difference between northern and southern transects (Bharathi et al., 2018; Gomes et al., 2000; Madhupratap et al., 2003). Upper layer Chl. *a* was high in inshore and LSPA influenced locations. Freshwater inputs bring the organic and inorganic nutrients supports the phytoplankton growth results the high Chl. *a* in adjacent coastal waters, similar results of high phytoplankton production in coastal waters especially near to river join locations of the BoB and Arabian Sea was reported by Amol et al. (2019); Bharathi et al. (2018); Madhu et al. (2006); Madhupratap et al. (2003). LSPA locations faced high Chl. *a* in upper layers, especially top 10m situations. High Chl. *a* with low salinity indicates the LSPA can significantly alter the biological production. This was further corroborated, as the RDA plots, LSPA influenced locations are in close assemblages with the decreasing gradients of the salinity and increasing gradients of the Temperature, DO and Chl. *a*. LSPA influenced locations, upper layer Chl. *a* was 2—5 folds high compared to adjacent locations.

As stated above, the SSCM was shallow and intense in the offshore regions of the northern bay compared to GD. This north-south difference was mainly due to cold-core eddy feature in the north and warm-core features in GD (Figures 2—4). The cold-core eddy, pumping the nutrients in the euphotic layer can lead to a high Chl. *a* (Jagadeesan et al., 2019; Jyothibabu et al., 2008; Prasanna Kumar et al., 2004; Sarma et al., 2018; Sarma et al., 2019) in northern transects. In contrast, the downwelling may deepen the nitro-cline, but relatively less PAR than the optimum levels in the high nutrients layers results the less Chl. *a*

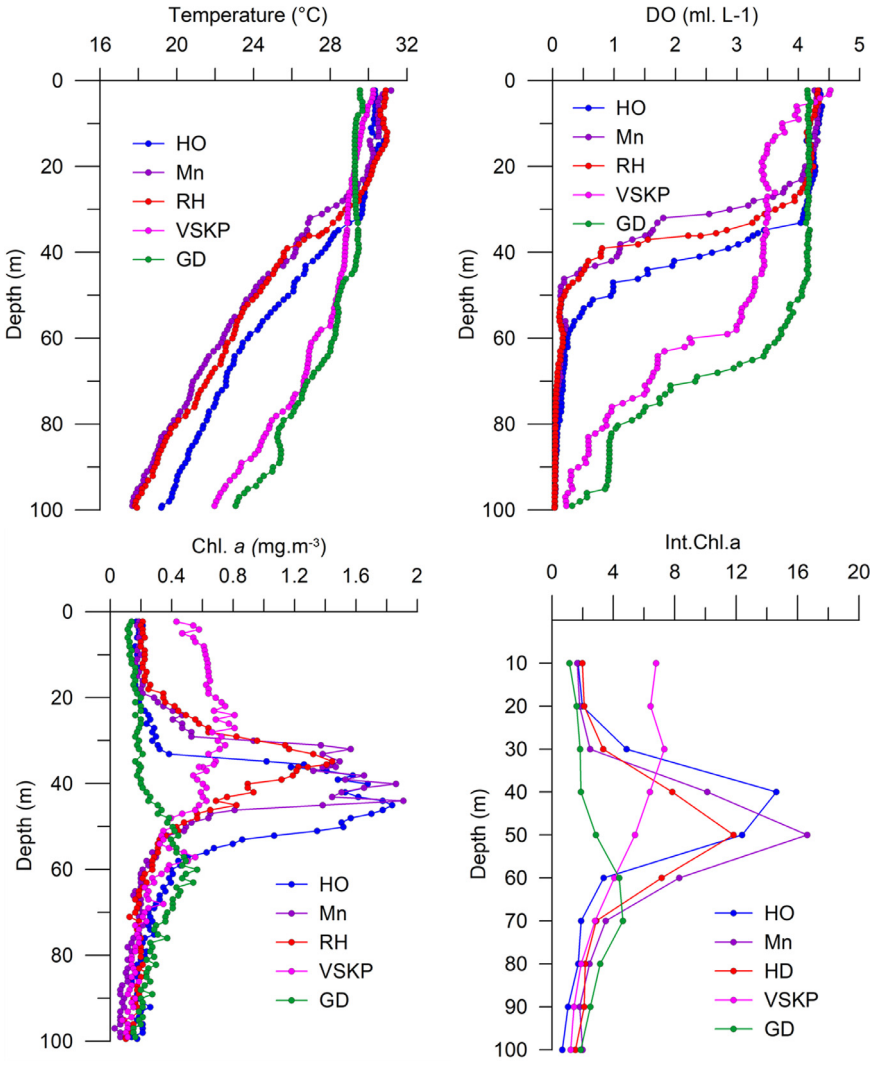

Figure 10 Offshore comparison of the temperature, Dissolved oxygen, Chlorophyll *a* and Integrated Chlorophyll *a* (mg m^{-2}) between transects. Northern transects are relatively warm and oxygen rich in upper layers, however subsurface layers (below 40 m) are warm and oxygenated in southern transects related with existing mesoscale physical processes [cold core features (up slopping) in northern transects and warm core (down slopping) features in the GD transects]. Subsurface Chlorophyll maxima (SSCM) were prominent and shallow in northern transects, however, SSCM were deeper and relatively have less Chlorophyll *a* in VSKP and GD.

(Jyothibabu et al., 2018; Sarma et al., 2018). Salinity stratification in upper layers restricts the cold core eddy pumping within subsurface layers results the low Chl. *a* in upper layers (Jagadeesan et al., 2019; Prasanna Kumar et al., 2004; Sarma et al., 2018).

The present observation could identify three types of Chlorophyll *a* distribution in the WBoB i) Surface Chlorophyll *a* Maxima (ii) Subsurface Chlorophyll *a* Maxima (iii) Double Chlorophyll *a* Maxima (Figures 6 and 7). SCM in the inshore and SSCM in the offshore region is a feature common to the BoB (Jyothibabu et al., 2008; Madhu et al., 2006; Madhupratap et al., 2003; Prasanna Kumar et al., 2004; Sarma and Aswanikumar, 1991; Sarma et al., 2018). However, presence of DoCM is reported first time in the BoB along the path of LSPA in the slope locations of MN and RK. DoCM is less known in the WBoB. DoCM in WBoB was first reported by Amol et al. (2019) in slope regions off Mahanadi due to freshwater plume from the North. This study DoCM found in the slope regions of MN and RK could be indicative of the southward advection of LSPA influencing the biological production along the path (>500 km).

Noticeably, the LSP influenced slope regions, subsurface chlorophyll maxima concentration was less than the offshore region. One of the reasons could be the relatively high turbidity of LSP locations that can reduce the light availability in the subsurface. In contrast, a relatively less turbid and nutrient-rich subsurface layer in shallow depth by cyclonic eddy features can support high Chl. *a* in the offshore region compared to LSP locations. An identical result on the influence of PAR and turbidity on SSCM is also available from the BoB (Jyothibabu et al., 2018). The overall pattern of the Multivariate RDA plots ordination explains hydrography and

Chl. *a* distribution in surface and column layers of the WBoB influenced by the combined action of the local inputs, LSPA (>500 km towards south) and existing physical processes. Eddies and EICC play a significant role in transporting the northern low saline Plume towards the south during the FIM period. LSPA was away from the shore and influencing the hydrobiology in their path. Local inputs of MN, RK alters the hydrography and Chl. *a* in inshore and near coastal locations and mesoscale physical processes influencing the offshore hydrography and phytoplankton production.

5. Summary and conclusion

The present study delineates the role of freshwater input from small and medium rivers, low saline advection and mesoscale eddies on the biological production in the WBoB. Riverine inputs from the Ganges and Brahmaputra results the formation of low saline plumes in the NWBoB. During the Late SWM or FIM low saline plume propagates towards the southward concordance with the EICC. EICC and mesoscale eddies jointly regulates the path of LSPA. LSP advection was directed towards the offshore by a cold-core eddy at ~18°N (> 500 km from north). LSPA is well separated from the local inputs. Mahanadi river influence in hydrography and biological production found up to near coast locations (~50 km), however in RK transect, this was into inshore location (~15 km). LSPA results the intermittent low salinity in upper layers (surface — 20 m) of HO, MN and RK. LSPA influenced location upper layer is low saline (2—10 units), warm, turbid, relatively nutrients and oxygen-rich than adjacent stations. Offshore station, subsurface layers were relatively cool, high saline, nutrients rich and less oxygenated in north transects compared to GD related with the existing mesoscale physical processes. Upper layer, Chl. *a* is relatively high in inshore and LSPA influenced locations (2-3 folds high) compared to adjacent stations. Along the HO, MN and RK transect, subsurface Chl. *a* maxima (SSCM) was shallow and prominent in the offshore regions compared to slope. High Chlorophyll *a* in the inshore, near coastal and LSPA influenced locations are suggestive of the possible role of riverine influx related inorganic and organic nutrients in the productivity cycle in the BoB. This study captured Double Chlorophyll *a* Maxima (DoCM) in LSPA influenced slope waters of MN and RK transect. DoCM less known pattern of Chl. *a* from WBOB. DoCM has both the surface maxima (surface — 10 m) and subsurface maxima (40—80 m); both layers were well separated by intermittent low Chl. *a* conditions. Inshore and coastal locations exhibited prominent surface maxima; offshore locations had prominent subsurface Chlorophyll *a* maxima. Slope region, influenced by LSP had a unique pattern of DoCM. In short, this study points out small and medium riverine inputs impacts hydrography and Chl. *a* around 10—50 km from the shore (inshore and near coastal locations). LSPA alters the hydrography and Chl. *a* along their path (>500 km). Existing mesoscale physical processes determines the column hydrography and Chl. *a* pattern across transects. This study is the first explains the combined details of the various processes influence on the cross-shore sectional hydrography and Chlorophyll *a* distribution in the western Bay of Bengal.

Declaration of competing interest

The authors declare that they have no known competing financial interests or personal relationships that could have appeared to influence the work reported in this paper.

Acknowledgement

The authors thank the Director, CSIR — National Institute of Oceanography, India, for facilities and encouragement. The authors thank the Scientist-in-Charge, CSIR NIO RC Visakhapatnam for encouragement and support. The authors thank Dr. V.V.S.S. Sarma, Dr. Amol Prakash, Dr. T.N.R. Srinivas and Dr. B.D. Shenoy from CSIR, NIO, RC, Visakhapatnam for their constant assistance and initial review of the manuscript. The authors thank all participants and the ship members who extended their help for the successful completion of the SSK 105 cruise. This is NIO contribution 6731.

References

Amol, P., Vinayachandran, P.N., Shankar, D., Thushara, V., Vijith, V., Chatterjee, A., Kankonkar, A., 2019. Effect of freshwater advection and winds on the vertical structure of Chlorophyll in the northern Bay of Bengal. Deep Sea Res. Pt. II: Top. Stud. Oceanogr. 104622. https://doi.org/10.1016/j.dsr2.2019.07.010

Antia, N.J., Harrison, P.J., Oliveira, L., 1991. The role of dissolved organic nitrogen in phytoplankton nutrition, cell biology and ecology. Phycologia 30, 1—89. https://doi.org/10.2216/i0031-8884-30-1-1.1

Baliarsingh, S.K., Lotliker, A.A., Sahu, K.C., Sinivasa Kumar, T., 2015. Spatio-temporal distribution of chlorophyll-a in relation to physico-chemical parameters in coastal waters of the northwestern Bay of Bengal. Environ. Monit. Assess. 187, art. 481. https://doi.org/10.1007/s10661-015-4660-x

Baliarsingh, S.K., Srichandan, S., Lotliker, A.A., Sahu, KC, Srinivasa Kumar, T., 2016. Phytoplankton community structure in local water types at a coastal site in northwestern Bay of Bengal. Environ. Monit. Assess. 188, art. 427. https://doi.org/10.1007/s10661-016-5424-y

Bharathi, M.D., Sarma, V.V.S.S., Ramaneswari, K., Venkataramana, V., 2018. Influence of river discharge on abundance and composition of phytoplankton in the western coastal Bay of Bengal during peak discharge period. Mar. Pollut. Bull. 133, 671—683. https://doi.org/10.1016/j.marpolbul.2018.06.032

Chaitanya, A.V.S., Lengaigne, M., Vialard, J., Gopalakrishna, V.V., Durand, F., Kranthikumar, C., Amritash, S., Suneel, V., Papa, F., Ravichandran, M., 2014. Salinity Measurements Collected by Fishermen Reveal a "River in the Sea" Flowing Along the Eastern Coast of India. Bull. Am. Meteorol. Soc. 95, 1897—1908.

Choudhury, A.K., Pal, R., 2011. Variations in seasonal phytoplankton assemblages as a response to environmental changes in the surface waters of a hypo saline coastal station along the Bhagirathi — Hooghly estuary. Environ. Monit. Assess. 179, 531—553. https://doi.org/10.1007/s10661-010-1761-4

Dyson, N., Jitts, H.R., Scott, B.D., 1965. Techniques for measuring oceanic primary production using radioactive carbon. Tech. Pap. 18. Division of Fisheries and Oceanography, CSIRO, Melbourne.

Fernandes, V., Ramaiah, N., 2009. Mesozooplankton community in the Bay of Bengal (India): spatial variability during the summer monsoon. Aquatic Ecol. 43, 951—963. https://doi.org/10.1007/s10452-008-9209-4

Gomes, H.R., Goes, J.I., Saino, T., 2000. Influence of physical processes and freshwater discharge on the seasonality of phytoplankton regime in the Bay of Bengal. Cont. Shelf Res. 20, 313—330. https://doi.org/10.1016/S0278-4343(99)00072-2

Gopalakrishna, V.V., Murty, V.S.N., Sengupta, D., Shenoy, S., Araligidad, N., 2002. Upper ocean stratification and circulation in the northern Bay of Bengal during southwest monsoon of 1991. Cont. Shelf Res. 22, 791—802. https://doi.org/10.1016/S0278-4343(01)00084-X

Grasshoff, K., 1983. Methods of Seawater Analysis. Weinheim, Verlag Chemie.

Jagadeesan, L., Kumar, G.S., Rao, D.N., babu, N.S., Srinivas, T.N.R., 2019. Role of eddies in structuring the mesozooplankton composition in coastal waters of the western Bay of Bengal. Ecol. Indi. 105, 137—155. https://doi.org/10.1016/j.ecolind.2019.05.068

Jyothibabu, R., Arunpandi, N., Jagadeesan, L., Karnan, C., Lallu, K.R., Vinayachandran, P.N., 2018. Response of phytoplankton to heavy cloud cover and turbidity in the northern Bay of. Bengal. Sci. Rep. 8, 11282. https://doi.org/10.1038/s41598-018-29586-1

Jyothibabu, R., Madhu, N.V., Maheswaran, P.A., Jayalakshmy, K.V., Nair, K.K.C., Achuthankutty, C.T., 2008. Seasonal variation of microzooplankton (20-200 μm) and its possible implications on the vertical carbon flux in the western Bay of Bengal. Cont. Shelf Res. 28, 737—755. https://doi.org/10.1016/j.csr.2007.12.011

Jyothibabu, R., Vinayachandran, P.N., Madhu, N.V., Robin, R.S., Karnan, C., Jagadeesan, L., Anjusha, A., 2015. Phytoplankton size structure in the southern Bay of Bengal modified by the Summer Monsoon Current and associated eddies: Implications on the vertical biogenic flux. J. Mar. Sys. 143, 98—119. https://doi.org/10.1016/j.jmarsys.2014.10.018

Krishna, M.S., Prasad, M.H.K., Rao, D.B., Viswanadham, R., Sarma, VVSS, Reddy, N.P.C., 2016. Export of dissolved inorganic nutrients to the northern Indian Ocean from the Indian monsoonal rivers during discharge period. Geochim. Cosmochim. Acta 172, 430—443. https://doi.org/10.1016/j.gca.2015.10.013

Kusum, K.K., Vineetha, G., Raveendran, T.V., Muraleedharan, K.R., Habeebrehman, H., Philson, K.P., Achuthankutty, C.T., 2018. River plume fronts and their implications for the biological production of the Bay of Bengal, Indian Ocean. Mar. Ecol. Prog. Ser. 597, 79—98. https://doi.org/10.3354/meps12607

Leps, J., Smilauer, P.S., 2003. Multivariate analysis of ecological data using CANOCA. Cambridge Univ. Press, Cambridge, UK.

Letscher, R.T., Hansell, D.A., Carlson, C.A., Lumpkin, R., Knapp, A.N., 2013. Dissolved organic nitrogen in the global surface ocean: Distribution and fate. Global Biogeochem. Cy. 27, 141—153. https://doi.org/10.1029/2012GB004449

Madhu, N.V., Jyothibabu, R., Maheswaran, P.A., John Gerson, V., Gopalakrishnan, T.C., Nair, K.K.C., 2006. Lack of seasonality in phytoplankton standing stock (Chlorophyll a) and production in the western Bay of Bengal. Cont. Shelf Res. 26, 1868—1883. https://doi.org/10.1016/j.csr.2006.06.004

Madhupratap, M., Gauns, M., Ramaiah, N., Prasanna Kumar, S., Muraleedharan, P.M., de Sousa, S.N., Sardessai, S., Muraleedharan, U., 2003. Biogeochemistry of the Bay of Bengal: physical, chemical and primary productivity characteristics of the central and western Bay of Bengal during summer monsoon 2001. Deep Sea Res. Pt. II Top. Stud. Oceanogr. 50, 881—896. https://doi.org/10.1016/S0967-0645(02)00611-2

Mahadevan, A., D'Asaro, E., Lee, C., Perry, M.J., 2012. Eddy—Driven Stratification Initiates North Atlantic Spring Phytoplankton Blooms. Science 337, 54—58.

Moschonas, G., Gowen, R.J., Paterson, R.F., Mitchell, E., Stewart, B.M., McNeill, S., Glibert, P.M., Davidson, K., 2017. Nitrogen dynamics and phytoplankton community structure: the role of organic nutrients. Biogeochemistry 134, 125—145. https://doi.org/10.1007/s10533-017-0351-8

Muraleedharan, K.R., Jasmine, P., Achuthankutty, C.T., Revichandran, C., Dinesh Kumar, P.K., Anand, P., Rejomon, G., 2007. Influence of basin-scale and mesoscale physical processes on biological productivity in the Bay of Bengal during the summer monsoon. Prog. Oceanogr. 72, 364—383. https://doi.org/10.1016/j.pocean.2006.09.012

Murty, V.S.N., Sarma, Y.V.B., Rao, D.B., Murty, C.S., 1992. Water characteristics, mixing and circulation in the Bay of Bengal during the Souhwest Monsoon period. J. Mar. Res. 50, 207—228.

Naik, S., Mishra, R.K., Panda, U.S., Mishra, P., Panigrahy, R.C., 2020. Phytoplankton Community Response to Environmental Changes in Mahanadi Estuary and Its Adjoining Coastal Waters of Bay of Bengal: a Multivariate and Remote Sensing Approach. Remote Sens. Earth Sys. Sci. 3, 110—122. https://doi.org/10.1007/s41976-020-00036-9

Paul, J.T., Ramaiah, N., Sardessai, S., 2008. Nutrient regimes and their effect on distribution of phytoplankton in the Bay of Bengal. Mar. Environ. Res. 66, 337—344. https://doi.org/10.1016/j.marenvres.2008.05.007ff

Prasad, 2014. Variability of dissolved organic matter in the Godavari estuary and western coastal Bay of Bengal: Influence of river discharge Ph.D. Thesis. Andhra University, India.

Prasanna Kumar, S., Muraleedharan, P.M., Prasad, T.G., Gauns, M., Ramaiah, N., de Souza, S.N., Sardesai, S., Madhupratap, M., 2002. Why is the Bay of Bengal less productive during summer monsoon compared to the Arabian Sea? Geophys. Res. Lett. 29, 88-81—88-84. https://doi.org/10.1029/2002GL016013

Prasanna Kumar, S., Nuncio, M., Narvekar, J., Kumar, A., Sardesai, S., De Souza, S.N., Gauns, M., Ramaiah, N., Madhupratap, M., 2004. Are eddies nature's trigger to enhance biological productivity in the Bay of Bengal? Geophys. Res. Lett. 31. https://doi.org/10.1029/2003GL019274

Prasanna Kumar, S., Nuncio, M., Ramaiah, N., Sardesai, S., Narvekar, J., Fernandes, V., Paul, J.T., 2007. Eddy-mediated biological productivity in the Bay of Bengal during fall and spring intermonsoons. Deep Sea Res. Pt. I: Oceanogr. Res. Pap. 54, 1619—1640. https://doi.org/10.1016/j.dsr.2007.06.002

Rao, R.R., Sivakumar, R., 2003. Seasonal variability of sea surface salinity and salt budget of the mixed layer of the north Indian Ocean. J. Geophys. Res. Oceans. 108, 9-1—9-14. https://doi.org/10.1029/2001JC000907

Sarma, V.V., Aswanikumar, V., 1991. Subsurface chlorophyll maxima in the northwestern Bay of Bengal. J. Plankton Res. 13, 339—352.

Sarma, V.V.S.S., Jagadeesan, L., Dalabehera, H.B., Rao, D.N., Kumar, G.S., Durgadevi, D.S., 2018. Role of eddies on intensity of oxygen minimum zone in the Bay of Bengal. Cont. Shelf Res. 168, 48—53. https://doi.org/10.1016/j.csr.2018.09.008

Sarma, V.V.S.S., Krishna, M.S., Rao, V.D., Viswanadham, R., Kumar, N.A., Kumari, T.R., Gawade, L., Ghatkar, S., Tari, A., 2012. Sources and sinks of CO_2 in the west coast of Bay of Bengal. Tellus B Chem. Phys. Meteorol. 64, 10961. https://doi.org/10.3402/tellusb.v64i0.10961

Sarma, V.V.S.S., Krishna, M.S., Viswanadham, R., Rao, G.D., Rao, V.D., Sridevi, B., Kumar, B.S.K., Prasad, V.R., Subbaiah, C.V., Acharyya, T., Bandopadhyay, D., 2013. Intensified oxygen minimum zone on the western shelf of Bay of Bengal during summer monsoon: influence of river discharge. J. Oceanogr. 69, 45—55. https://doi.org/10.1007/s10872-012-0156-2

Sarma, VVSS, Rao, D.N., Rajula, G.R., Dalabehera, H.B., Yadav, K., 2019. Organic Nutrients Support High Primary Production in the Bay of Bengal. Geophys. Res. Lett. 46, 6706—6715. https://doi.org/10.1029/2019GL082262

Shankar, D., Vinayachandran, P.N., Unnikrishnan, AS, 2002. The monsoon currents in the north Indian Ocean. Prog. Oceanogr. 52, 63—120. https://doi.org/10.1016/S0079-6611(02)00024-1

Shenoy, S.S.C., 2010. Intra-seasonal variability of the coastal currents around India: A review of the evidences from new observations. Indian J. Geo-Mar. Sci. 39, 489—496.

Shetye, S.R., 1993. The movement and implications of the Ganges-Bramhaputra runoff on entering the Bay of Bengal. Curr. Sci. 64, 32—38.

Shetye, S.R., Gouveia, A.D., Shankar, D., Shenoi, S.S.C., Vinayachandran, P.N., Sundar, D., Michael, G.S., Nampoothiri, G., 1996. Hydrography and circulation in the western Bay of Bengal during the northeast monsoon. J. Geophys. Res. - Oceans. 101, 14011—14025. https://doi.org/10.1029/95JC03307

Shetye, S.R., Shenoi, S.S.C., Gouveia, A.D., Michael, G.S., Sundar, D., Nampoothiri, G., 1991. Wind-driven coastal upwelling along the western boundary of the Bay of Bengal during the southwest monsoon. Cont. Shelf Res. 11, 1397—1408. https://doi.org/10.1016/0278-4343(91)90042-5

Subramanian, V., 1993. Sediment load of Indian Rivers. Curr. Sci. 64, 928—930.

UNESCO, 1994. Protocols for the Joint Global Ocean Flux studies (JGFOS). Core measuremens, IOC Manual and Guides. UNESCO, Paris.

Varkey, M.J., Murty, V.S.N., Suryanarayana, A., 1996. Physical oceanography of the Bay of Bengal and Andaman Sea. Oceanogr. Mar. Biol. — Annual Rev. 34, 1—70.

Vinayachandran, P.N., Kurian, J., 2007. Hydrographic observations and model simulation of the Bay of Bengal freshwater plume. Deep Sea Res. Pt. I - Oceanogr. Res. Pap. 54, 471—486. https://doi.org/10.1016/j.dsr.2007.01.007

Vinayachandran, P.N., Murty, V.S.N., Ramesh Babu, V., 2002. Observations of barrier layer formation in the Bay of Bengal during summer monsoon. J. Geophys. Res. Oceans 107 C (12), 8018. https://doi.org/10.1029/2001JC000831

Zar, J.H., 1999. Biostatistical analysis, 4th edn. Prentice-Hall, Upper Saddle River.